TeV Measurements of Objects from the Fermi Bright Source List with Milagro

John Pretz* for the Milagro Collaboration

**Los Alamos National Lab*

Abstract. **The Fermi Gamma-ray Space Telescope has released a list of the most significant 205 sources with three months of Fermi data. The Milagro Gamma-Ray Observatory is sensitive to gamma-rays above 100 GeV, overlapping and extending the energy range of Fermi. Of the Galactic Fermi sources in the field of view of Milagro, 14 Fermi sources are observed at greater than 3 sigma. Of these 14 sources, 9 are pulsars and 9 have never been detected at TeV energies. Milagro measurements will be presented, emphasizing the broad-band (100 MeV to 100 TeV) behavior of these sources.**

Keywords**: VHE Gamma Rays,Fermi,Milagro**

I. INTRODUCTION

The Milagro experiment was a water-Cherenkov air shower array operating at a latitude of 35.88N in the Jemez mountains above Los Alamos, NM [1], [2], [3]. The central Milagro water pond contained two layers of photo-multiplier tubes (PMTs), the bottom of which was used to distinguish the penetrating component characteristic of hadronic air showers. This capability gives some capacity to distinguish cosmic-ray induced air showers from gamma-ray induced showers.

The Fermi Bright Source List (BSL) is a list of 205 high-confidence detections between 100 MeV and 100 GeV by the Fermi Large Area Telescope (Fermi-LAT) [4]. The BSL was originally conceived as a tool for preparing proposals for the second round of the Guest Investigator program, but the BSL has great scientific merit representing a deeper survey of the 100 MeV to 100 GeV sky in three months than all of EGRET data. Of particular note, the BSL includes new pulsar detections where, for the first time, pulsed emission has been discovered first in the 100 MeV - 100 GeV energy range.

This paper describes the results of a search of Milagro data for statistical excesses from potential Galactic sources in the Fermi Bright Source List (BSL). Of the 205 sources in the BSL, 34 are in the field of view of Milagro and are not identified as extra-galactic sources. Of these 34 Fermi sources, 14 are observed in Milagro data at greater than 3σ.

II. FERMI BRIGHT SOURCE LIST SEARCH

We conduct a search of the Milagro data using a newly-optimized analysis which differs from previous analyses by optimizing the event gamma/hadron weighting as a function of the size of the event. This approach, combined with an additional year and a half of data, gives a 15% to 25% increase in the search sensitivity, depending on the spectrum of the source. This analysis weights high-energy events somewhat more strongly than previous analyses and we expect a median energy near 35 TeV for a crablike spectrum with no cutoff.

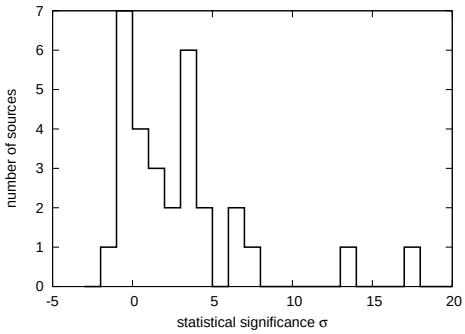

Fig. 1. Distribution of the significances of the 34 potential Galactic sources in the field of view of Milagro. The distribution is well described by a Gaussian for sources up to about σ of 3 at which point we observe a long tail to high significance. Most of the sources between 3σ and 5σ are TeV-scale emitters, but they are too dim to identify unambiguously individually.

We select 34 sources of the 205 sources in the BSL. Sources are selected which are in the field of view of Milagro (defined as a Declination, δ, greater than -5°). We choose sources which have not been positively identified as extra-Galactic sources in the BSL because this Milagro analysis has a high expected median energy and is less sensitive to extra-Galactic emission because of absorbtion of multi-TeV photons by the extra-Galactic Background Light. Of the 34 selected sources, 16 have been identified as pulsars in the BSL by measurements of pulsed emission in the Fermi data. One is a high-mass X-ray binary. Five have a potential association with supernova remnants, but that association is based solely on similar locations, and 12 of the selected BSL sources have no clear association.

III. RESULTS

Of the 34 sources included in the search, 14 are observed in the Milagro data at the position of the Fermi-LAT source at or above 3 standard deviations above the cosmic-ray background. Figure 1 summarizes the significances observed. Because of so many 3σ excesses, a pure background origin for these excesses, taken as a whole, is excluded at more than 5σ; the probability of 4 or more excesses at or above 3σ is $\sim 1.5\times10^{-7}$. Even

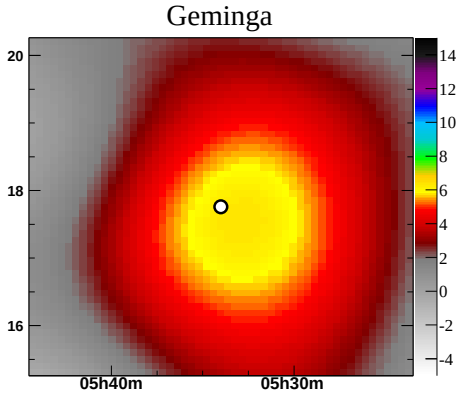

Fig. 2. Milagro significance map around Geminga, indicated with a white dot. The data has been prepared by smoothing with a 1° Gaussian convolved with the detector point spread function in order to search for regions of extended emission.

allowing for the 6 sources in the BSL which are at or near locations of previously reported Milagro results, we can still say that most of the remaining 14 Fermi sources are seen in Milagro data. The results of the search are summarized in Table I. For each Fermi source in Table I at or above 3σ, we give the measured flux implied by the Milagro measurements. We calculate the flux by comparing the measured number of events to simulation expectation under the assumption that the spectrum is $\propto E^{-2.6}$. The systematic error in the measured flux due to using this assumed spectrum rather than the true spectrum is minimized if we quote the flux at the median energy of the assumed spectrum. We quote the differential flux at 35 TeV which is the simulation-expected median energy for an $E^{-2.6}$ spectrum. This technique for estimating the flux is expected to introduce some 20% systematic error in the quoted fluxes in addition to an approximately 30% error due to variations in the trigger rate.

Figure 3 shows the significance in the Milagro data for regions surrounding the 14 Fermi sources above 3σ in the Milagro data. Of the 34 searched sources, 16 are identified by Fermi as pulsars and we observe 9 in the Milagro data at or above 3σ. We observe 3 of 5 Fermi sources associated with known supernova remenants, and we observe 2 of 13 sources with no known identification. It is striking how frequently the 100 MeV to 100 GeV emission reported by Fermi is associated with emission in the TeV range for pulsars and SNR. All 6 of the sources previously reported by Milagro which are included in the BSL are now associated with 100 MeV - 100 GeV pulsars. A picture is emerging where the typical TeV-scale source is associated with lower-energy pulsars suggesting that the typical TeV-scale source is a pulsar wind nebula. We also note that 6 of the sources seen at 3σ or more in Milagro data have never been associated with TeV-scale emission before.

IV. Discussion

Some of the sources shown in Figure 3 bear special note.

0FGL 0634.0+1745 is the Geminga pulsar, the brightest source in the BSL in the field of view of Milagro. It was reported previously by the Milagro collaboration as C3 in the first survey of the Galactic plane. The location of the Fermi source is observed at 3.5σ in the Milagro data, but if we smooth the data by a 1° Gaussian in addition to the normal smoothing by the Milagro point-spread function, the significance goes up to 6.3σ, as seen in Figure 2. We fit a Gaussian to the unsmoothed data and determine a full width at half maximum of the region as $2.6^{+0.7}_{-0.9}{}^\circ$, after accounting for the point spread function. This suggests a size for the emission region of 5 to 10 pc, consistent with Imaging Atmospheric Cherenkov Telescope mesurements of more distant PWN. Given that the Geminga pulsar is so nearby (an estimated 169 pc), we would expect it to appear this large on the sky.

0FGL J2032.2+4122 and **0FGL J2021.5+4026** are two pulsars in which the pulsations were identified first by the LAT. These two pulsars are coincident with the previously-reported Milagro source MGRO J2031+41. It is interesting to note the the original Milagro detection identified this region as one source with a 3° spatial extent. With the Fermi data as a guide, it appears that there may be in fact two TeV sources in this region.

0FGL J1907.5+0602 is associated with MGRO J1908+06. This source is noteworthy as the first Milagro-identified source to be subsequently confirmed by an IACT with an extent measured by HESS as $0.21^{+0.07}_{-0.05}{}^\circ$ [5]. The Fermi source is a LAT-identified pulsar. The peak of the Milagro detection is 0.3° from the location of the pulsar, but is consistent within measurement error.

0FGL J2229.0+6114 is coincident with the radio pulsar J2229+6114. The source has been already associated with a Milagro candidate C4 from the first Milagro survey of the Galactic plane. We observe a 6.6σ excess at the position of the LAT pulsar. With the additional data and improved analysis technique, this source is elevated to a high-confidence detection of TeV emission.

References

[1] A. Abdo et al. ApJL. **658**. L33. (2007)
[2] A. Abdo et al. ApJL. **664**. L91. (2007)
[3] A. Abdo et al. ApJL. **688**. 1078. (2008)
[4] A. Abdo et al. ApJS (submitted). arXiv:0902.1340.
[5] A. Djannati-Atai et al. Proc. 30th ICRC. **2**. 831. (2007)

TABLE I
SUMMARY OF THE MILAGRO DATA AT FERMI BSL LOCATIONS. THE SOURCE NAME IN THE BSL, IT'S LOCATION ARE INDICATED ALONG WITH THE MILAGRO FLUX OR FLUX LIMIT, THE SOURCE SIGNIFICANCE IN THE MILAGRO DATA AND ANY KNOWN TEV ASSOCIATIONS. FLUXES ARE SPECIFIED IN UNITS OF 10^{-17}TeV cm^{-2}sec^{-1}

Name	Type	RA(deg)	Dec.(deg)	Gal. Long. (deg)	Gal. Lat(deg)	flux	Significance	TeV Associations
J0007.4+7303	PSR	1.85	73.06	119.69	10.47	< 90.4	2.6	
J0030.3+0450	PSR	7.60	4.85	113.11	-57.62	< 20.9	-1.7	
J0240.3+6113	HXB	40.09	61.23	135.66	1.07	< 26.2	0.7	LSI +61 303
J0357.5+3205	PSR	59.39	32.08	162.71	-16.06	< 16.5	-0.1	
J0534.6+2201	PSR	83.65	22.02	184.56	-5.76	162.6 ± 9.4	17.2	Crab
J0613.9-0202	PSR	93.48	-2.05	210.47	-9.27	< 60.0	-0.0	
J0617.4+2234	SNR[a]	94.36	22.57	189.08	3.07	28.8 ± 9.5	3.0	IC443
J0631.8+1034	PSR	97.95	10.57	201.30	0.51	47.2 ± 12.9	3.7	
J0633.5+0634	PSR	98.39	6.58	205.04	-0.96	< 50.2	1.4	
J0634.0+1745	PSR	98.50	17.76	195.16	4.29	37.7 ± 10.7	3.5	MGRO C3 Geminga
J0643.2+0858		100.82	8.98	204.01	2.29	< 30.5	0.3	
J1653.4-0200		253.35	-2.01	16.55	24.96	< 51.0	-0.5	
J1830.3+0617		277.58	6.29	36.16	7.54	< 32.8	0.2	
J1836.2+5924	PSR	279.06	59.41	88.86	25.00	< 14.6	-0.9	
J1844.1-0335		281.04	-3.59	28.91	-0.02	148.4 ± 34.2	4.3	
J1848.6-0138		282.16	-1.64	31.15	-0.12	< 91.7	1.7	
J1855.9+0126	SNR[a]	283.99	1.44	34.72	-0.35	< 89.5	2.2	
J1900.0+0356		285.01	3.95	37.42	-0.11	70.7 ± 19.5	3.6	
J1907.5+0602	PSR	286.89	6.03	40.14	-0.82	116.7 ± 15.8	7.4	MGRO J1908+06 HESS J1908+063
J1911.0+0905	SNR[a]	287.76	9.09	43.25	-0.18	< 41.7	1.5	
J1923.0+1411	SNR[a]	290.77	14.19	49.13	-0.40	39.4 ± 11.5	3.4	HESS J1923+141
J1953.2+3249	PSR	298.32	32.82	68.75	2.73	< 17.0	0.0	
J1954.4+2838	SNR[a]	298.61	28.65	65.30	0.38	37.1 ± 8.6	4.3	
J1958.1+2848	PSR	299.53	28.80	65.85	-0.23	34.7 ± 8.6	4.0	
J2001.0+4352		300.27	43.87	79.05	7.12	< 12.1	-0.9	
J2020.8+3649	PSR	305.22	36.83	75.18	0.13	108.3 ± 8.7	12.4	MGRO J2019+37
J2021.5+4026	PSR	305.40	40.44	78.23	2.07	35.8 ± 8.5	4.2	
J2027.5+3334		306.88	33.57	73.30	-2.85	< 16.0	-0.2	
J2032.2+4122	PSR	308.06	41.38	80.16	0.98	63.3 ± 8.3	7.6	TEV 2032+41 MGRO J2031+41
J2055.5+2540		313.89	25.67	70.66	-12.47	< 17.6	-0.0	
J2110.8+4608		317.70	46.14	88.26	-1.35	< 24.1	1.1	
J2214.8+3002		333.70	30.05	86.91	-21.66	< 20.7	0.6	
J2229.0+6114	PSR	337.26	61.24	106.64	2.96	70.9 ± 10.8	6.6	MGRO C4
J2302.9+4443		345.75	44.72	103.44	-14.00	< 13.2	-0.6	

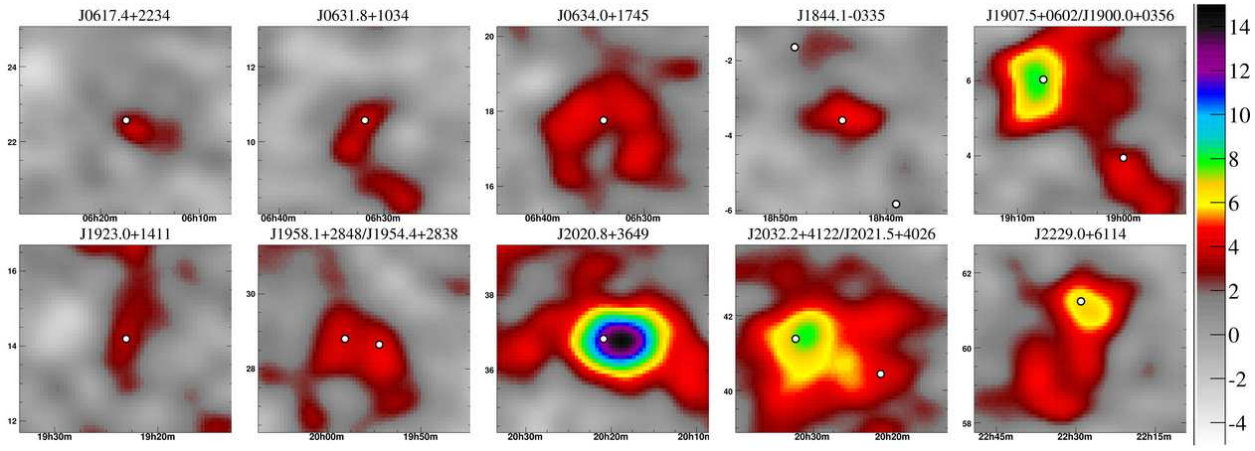

Fig. 3. The 3σ sources from Table I, omitting the Crab. Each frame shows a 5°x5° region with the LAT source positions indicated by white dots. The error on the Fermi source locations is quite small on this scale, typically between 0.1 and 0.2 degrees, depending on the source. The data has been smoothed by a Gaussian of width varying between 0.4° and 1.0°, depending on the expected angular resolution of events. Horizontal axes show Right-Ascension and vertical axes show Declination. The colors indicate the statistical significance in standard deviations.